

PCCP

Accepted Manuscript



This is an *Accepted Manuscript*, which has been through the Royal Society of Chemistry peer review process and has been accepted for publication.

Accepted Manuscripts are published online shortly after acceptance, before technical editing, formatting and proof reading. Using this free service, authors can make their results available to the community, in citable form, before we publish the edited article. We will replace this *Accepted Manuscript* with the edited and formatted *Advance Article* as soon as it is available.

You can find more information about *Accepted Manuscripts* in the [Information for Authors](#).

Please note that technical editing may introduce minor changes to the text and/or graphics, which may alter content. The journal's standard [Terms & Conditions](#) and the [Ethical guidelines](#) still apply. In no event shall the Royal Society of Chemistry be held responsible for any errors or omissions in this *Accepted Manuscript* or any consequences arising from the use of any information it contains.

Effect of Gamma Irradiation on Poly(vinylidene difluoride)-Lithium Bis(oxalato)borate Electrolyte

Mimi Hayati Abdul Rahaman¹, Mayeen Uddin Khandaker¹, Ziaul Raza Khan², Mohd Zieauddin Kufian³, Ikhwan Syaifiq Mohd Noor³, Abdul Kariem Arof^{3*}

¹Applied Radiation Laboratory, ²Low Dimensional Materials Research Centre, ³Centre for Ionics University of Malaya, Department of Physics, Faculty of Science, University of Malaya, 50603 Kuala Lumpur, Malaysia.

*Corresponding Author: akarof@um.edu.my

Tel.: +60379674085

Fax : +60379674146

ABSTRACT

A poly(vinylidene difluoride) – lithium bis(oxalato)borate solid polymer electrolyte prepared by solvent casting method has been irradiated with different doses of gamma-rays. Differential scanning calorimetry reveals that the polymer electrolyte irradiated with 35 kGy of γ -rays is the most amorphous sample. This is also supported by results from X-ray diffraction. The fourier transform infrared spectrum of each irradiated sample has been deconvoluted in the wavenumber region between 1830 and 1758 cm^{-1} in order to predict the percentage of free and contact ions in the samples. The sample exposed to 35 kGy of γ -rays contains the highest percentage of free ions and the lowest amount of contact ions. This sample also exhibits the highest room temperature conductivity of $3.05 \times 10^{-4} \text{ S cm}^{-1}$, which is 15% higher relative to the virgin sample. The number density of free ions is observed to have more control on the conductivity variation with γ -radiation dose compared to ionic mobility. This study confirms that γ -irradiation can be a potential way to obtain highly conductive and mechanically stable polymer electrolytes.

Keywords: PVDF; LiBOB; Gamma Irradiation; ionic mobility; number density of charge carriers.

1. Introduction

Use of radiation in the study on polymer electrolytes has great importance because it helps in achieving some desired improvements in the properties of the electrolytes. The irradiation of polymeric materials with ionizing radiation leads to the formation of very reactive intermediate products such as excited states, ions and free radicals which can result in rearrangements or formation of new bonds [1]. The degree of these transformations depends on the structure of the polymer and the conditions of treatment before, during and after irradiation. Thorough control of all of these factors facilitates the modification of polymers by radiation processing. Nowadays, the modification of polymers covers radiation cross-linking, radiation induced polymerization (graft polymerization and curing) and the degradation of polymers.

Radiation can penetrate a polymer, break the polymer chains and create free radicals. These free radicals may create crosslinks with adjacent molecules and recombine. Generally, materials having cross-linked condition show long term performances in various aspects. Often the two processes (degradation-crosslinking) occur simultaneously, and the outcome of the process is determined by a competition between the reactions [1-2]. Oxidation and degradation occur gradually with increasing radiation dose. Different polymer electrolytes have different effects to radiation depending on the chemical bonds in the polymers. Different studies on the effect of ionization radiation on polymers reveal a variety of structural modifications such as main chain scission, intermolecular crosslinking, creation of unsaturated bonds, formation of volatile fragments and creation of carbonaceous clusters [3-4]. Gamma irradiation treatment provides a unique way to modify the chemical, structural, optical, mechanical and electrical properties of the polymer by causing irreversible changes in their macromolecular structure [5-

6]. Such irradiations may produce electrons and low energy photons which are responsible for the modification of the material.

Radiation also affects dielectric properties that are of particular interest to science and technology since dielectrics have many applications in modern engineering [7-10]. The effect of ionization radiation on dielectric properties of polymers has been studied by several workers [11-13]. The dielectric property has been found to depend strongly on the degree of crystallinity as well as on the manner in which a particular degree of crystallinity has been attained [14-16]. It is well known that irradiation treatment enhances the electrical conductivity in insulating polymers. This increase in ionic conductivity is because of fairly great electron freedom. In many researches it is found that the polymer electrolyte breaks down at very high radiation doses. However the threshold dose which a polymer is able to withstand before breakdown depends greatly on the chemical structure of the polymers. Indeed, below the destructive level of exposure, radiation treatment can impart numerous benefits to the polymer systems and enhance their properties [17-18].

Over the last four decades, ion-conducting polymers have been tremendously studied due to their potential application as the electrolytes in electrochemical devices. Various efforts have been devoted to develop polymer electrolytes (PE) since liquid electrolytes (LE) are known to give problems in devices [19]. As lithium-ion batteries continue to penetrate the battery market especially those related to portable gadgets such as notebook computers, camcorders, and telecommunication equipment, there is intense research and development efforts toward raising the technology performance. LiBOB meets a number of criteria required of salts for lithium-ion cells: (i) ability to form a stable solid electrolyte interphase (SEI) layer; (ii) good stability over a wide potential window; (iii) acceptable solubility in alkyl carbonate solvents such as ethylene

carbonate (EC), propylene carbonate (PC), and so forth; (iv) high conductivity in various aprotic solvents; and (v) ability to sustain a good cycling [20]. Thus, the use of a salt such as lithium bis(oxalato)borate (LiBOB) was chosen in this work.

Poly(vinylidene difluoride) or PVDF is suggested as the polymer host in this work. PVDF based polymer electrolyte with LiBOB salt was prepared by solution casting technique. PVDF is a widely studied semi crystalline polymer. The PVDF films, as well as their intrinsic physical properties, have been the subject of numerous publications [21-24]. In this communication, we report the effects of gamma irradiation on the ionic conductivity of a PVDF-LiBOB polymer electrolyte system. The γ -radiation dose was varied from 10 to 50 kGy. The changes produced by the induced γ -rays (if any) are detected through differential scanning calorimetry (DSC), fourier transform infrared (FTIR) spectroscopy and impedance spectroscopy (IS). Although a lot of work has been done to investigate the effect of γ -irradiation on PVDF polymer but the dependence of the investigated parameters related to polymer electrolytes due to γ -irradiation has not been completely understood so far. It is the aim of this paper to shed some light on conductivity variation with increasing doses of γ -radiation.

2. Experimental

2.1. Sample preparation

The analytical grade poly(vinylidene difluoride) or PVDF ($M_w = 2.7 \times 10^5 \text{ g mol}^{-1}$), lithium bis(oxalato)borate (LiBOB) and N-Methyl-2-pyrrolidone (NMP) have been used for sample preparation. The electrolyte polymer films have been prepared by the solution casting technique. 1 g of PVDF was dissolved in 15 mL NMP as a solvent. The mixture was stirred at 60°C until a homogenous solution was obtained. 30wt% of LiBOB salt was added into the solution and

stirring was continued for another 2 h. The homogeneous solution was then cast into a glass petri dish and dried at 60°C in a vacuum oven for 1 to 2 days to form free standing films.

2.2. *Gamma irradiation*

The samples were irradiated in air in a conventional gamma chamber at the Applied Radiation Laboratory, University of Malaya, using a cobalt-60 (^{60}Co) source with a dose rate of 3.34 Gy min⁻¹. The samples were exposed to γ -ray doses of 10, 25, 35, 40 and 50 kGy.

2.3. *Differential Scanning Calorimetry (DSC)*

DSC was carried out using DSC Q200 equipment from TA instruments to determine the glass transition temperature (T_g) and melting temperature (T_m) of non-irradiated and irradiated samples. About ~5 mg of the sample was sealed in aluminum pans and heated from -90 to 190 °C under a nitrogen flow at a heating rate of 10 °C min⁻¹.

2.4. *X-Ray Diffraction (XRD)*

XRD was carried out to determine the effect of gamma radiation on the crystalline/amorphous nature of the samples. X-Ray diffractograms of all samples were recorded using Olympus BTX Benchtop diffractometer from 2 theta angle of 5° to 45°.

2.5. *Fourier Transform Infrared (FTIR) Spectroscopy*

The effect of gamma radiation on the structure of the samples can be determined using FTIR. Thermo Scientific model Nicolet iS10 spectrometer was used to record the IR spectra of the samples. The spectrum was recorded in the transmittance mode between 650 and 4000 cm⁻¹ with resolution of 4 cm⁻¹.

2.6. Impedance Spectroscopy

Impedance measurement was performed using the HIOKI 3532-50 LCR Hi-Tester in the frequency ranges from 50 Hz to 5 MHz. The sample was sandwiched between two stainless steel blocking electrodes of 2 cm diameter and measured at room temperature (278K). A graph of negative imaginary impedance against real impedance was then plotted. The bulk resistance, R_b was obtained from the intercept of the plot with the real impedance axis. The conductivity, σ of the sample was calculated using the following equation:

$$\sigma = \frac{t}{A \times R_b} \quad (1)$$

Here t is the sample thickness and A is the electrode-electrolyte contact area.

3. Results and discussions

3.1. Differential Scanning Calorimetry (DSC)

The DSC thermograms of PVDF-LiBOB electrolytes with different γ -radiation doses are shown in Fig. 1. The thermal properties of polymer electrolyte showed significant changes in the melting temperature, T_m upon γ -irradiation. The T_m of virgin samples is observed at 157.5°C. Irradiating the samples with γ -radiation up to 35 kGy gradually decreased the T_m of the sample. Beyond this dose of γ -radiation, the T_m of the sample is observed to increase. T_m is related with the degree of crystallinity. It has been reported that the shift of T_m towards lower temperature increases the amorphousness of the sample [25]. This can be estimated by calculating the relative degree of crystallinity, χ_c from the enthalpy of the melting of the sample using the equation (2):

$$\chi_c (\%) = \frac{\Delta H_m}{\Delta H_m^0} \times 100 \% \quad (2)$$

Here ΔH_m is the melting enthalpy of the sample and ΔH_m^0 is the melting enthalpy of the polymer host. In this work, the non-irradiated sample is considered 100% crystalline ($\Delta H_m^0 = 777.1 \text{ J g}^{-1}$) so that the variation of degree of crystallinity can be easily determined. Table 1 lists the thermal parameters and relative degree of crystallinity of all samples.

Fig. 1. The melting point, T_m peaks of PVDF-LiBOB electrolyte with different γ -radiation doses. Inset figure exhibits the DSC of PVDF-LiBOB polymer electrolyte in full scale cycles.

Table 1. T_g , T_m , ΔH_m and χ_c values of PVDF-LiBOB electrolytes with different γ -radiation doses.

From Table 1, the sample which is most amorphous is represented by the lowest degree of crystallinity. The sample irradiated with 35 kGy γ -rays showed the lowest crystallinity. The decrease in crystallinity may be due to the scissoring of polymer bonds on γ -irradiation resulting in increase in disorder and amorphousness of the polymer electrolyte.

The DSC thermogram shows glass transition temperature (T_g) of PVDF-LiBOB electrolyte with different γ -radiation doses are illustrated in Fig. 2. The T_g of virgin PVDF-LiBOB electrolyte is observed at -22.66°C . Irradiating the virgin PVDF-LiBOB electrolyte up to 35 kGy γ -rays decreased the T_g values to -58.17°C . Evidence from semi crystalline synthetic polymers showed that as the degree of crystallinity increased, the T_g also increased [26]. Conversely, as the ratio of amorphous to crystalline regions increased, T_g should decrease. The samples irradiated with 40 to 50 kGy γ -rays exhibited an increase in T_g from -36.74 to -36.09°C . This inferred that increase in gamma dose can initiate polymer cross-linking. Polymer cross-linking can result in

increase in localized crystallinity that can impede ionic mobility and lead to a decrease in conductivity.

Fig. 2. Glass transition temperature, T_g of PVDF-LiBOB electrolyte with (a) 0, (b) 10, (c) 25, (d) 35, (e) 40 and (f) 50 kGy γ -irradiation.

3.2. X-ray diffraction (XRD)

XRD is a powerful technique to study the structure of the present samples. LiBOB salt, non-irradiated and irradiated X-ray diffraction patterns of PVDF-LiBOB complexes with different γ -radiation doses are shown in Fig. 3. It is reported that PVDF semi crystalline polymer have four crystalline peaks centered at 2θ angle of 18.2° [100], 19.8° [020], 26.6° [110] and 38.6° [021] [27]. The complexation between PVDF polymer and LiBOB salt shifts the position of crystalline peaks of PVDF and the characteristic peaks due to LiBOB salt can be observed by deconvoluting the XRD diffractogram of PVDF-LiBOB electrolytes.

Fig. 3. XRD patterns of (a) LiBOB salt and PVDF-LiBOB electrolyte with PVDF-LiBOB electrolyte with (b) 0, (c) 10, (d) 25, (e) 35, (f) 40 and (g) 50 kGy γ -irradiation.

Fig. 4 shows the XRD deconvolution of PVDF-LiBOB electrolyte with different gamma irradiation. The crystalline peaks of PVDF are observed at $2\theta = \sim 18.5^\circ$, $\sim 20.6^\circ$, $\sim 26.7^\circ$ and $\sim 39.1^\circ$. The other sharp and narrow peaks observed at $2\theta = \sim 7.4^\circ$, $\sim 14.7^\circ$, $\sim 16.5^\circ$, $\sim 20.3^\circ$, $\sim 25.5^\circ$, $\sim 30.0^\circ$, $\sim 31.3^\circ$, $\sim 36.0^\circ$, $\sim 36.8^\circ$, $\sim 37.9^\circ$ and $\sim 39.1^\circ$ are the crystalline peaks of LiBOB salts [28]. The broad halos at $2\theta = \sim 19.8^\circ$ and $\sim 36.1^\circ$ represent the amorphous phase of the samples. The shifts in crystalline peak position of PVDF from that reported in [27] to that observed in Fig. 4 indicate the formation of polymer-salt complexes.

Fig. 4. XRD deconvolution of PVDF-LiBOB electrolyte with (a) 0, (b) 10, (c) 25, (d) 35, (e) 40 and (f) 50 kGy γ -irradiation.

The degree of crystallinity of the sample can also be determined from XRD deconvolution. The degree of crystallinity, χ_c can be calculated using the equation (3) [29]:

$$\chi_c(\%) = \frac{A_c}{A_c + A_a} \times 100\% \quad (3)$$

Here, A_c is area under the peaks representing total crystalline region and A_a is area under the peaks representing total amorphous region. Table 2 lists the values of A_c , A_a and χ_c of PVDF-LiBOB electrolytes with different γ -irradiation. It is observed that increasing the gamma irradiation up to 35 kGy increases the amorphous nature of the electrolyte. Beyond this gamma irradiation, the sample becomes more crystalline.

Table 2. A_c , A_a and χ_c values of PVDF-LiBOB electrolytes with different γ -radiation doses.

3.3 FTIR Spectrum

Radiation induces structural changes in polymers and infrared absorption (FTIR) spectroscopy is one of the analytical techniques used for the study of such changes in these systems. The FTIR spectra of non-irradiated and irradiated PVDF-LiBOB complexes between 1500 and 800 cm^{-1} for doses of 0, 10, 25, 35, 40 and 50 kGy are shown in Fig. 5. Table 3 lists the main FTIR peaks of PVDF-LiBOB and their possible assignments [30].

Fig. 5. FTIR Spectra of PVDF-LiBOB electrolyte with different γ -doses.

Table 3. The main FTIR peaks of PVDF-LiBOB and their possible assignments.

It is reported that exposing PVDF to γ -irradiation increases the intensity of the polymer peaks [31]. This can be proven by considering the band assigned to PVDF characteristics between 1220 and 1135 cm^{-1} . Fig. 6 shows the FTIR deconvolution of PVDF-LiBOB electrolyte with different γ -ray irradiation. The band at $\sim 1153 \text{ cm}^{-1}$ is assigned to PVDF [32]. Band at 1169 cm^{-1} and $\sim 1202 \text{ cm}^{-1}$ are assigned to $\nu_s(\text{CF}_2) + t(\text{CH}_2)$ and $\nu_a(\text{CF}_2) + w(\text{CF}_2)$ of PVDF, respectively [30]. The band at $\sim 1190 \text{ cm}^{-1}$ is assigned to C-O valence out-of phase of LiBOB salt. It is observed that the irradiation of 10 kGy gamma dose into the PVDF-LiBOB electrolyte increased the intensity of PVDF characteristic bands. The intensity of the three bands at ~ 1153 , ~ 1169 and $\sim 1202 \text{ cm}^{-1}$ keeps increasing with increasing gamma doses until a maximum is achieved for the electrolyte irradiated with 35 kGy of gamma radiation. Beyond this radiation dose, the intensity of the bands is observed to decrease. The intensity and area of the band due to LiBOB characteristics at $\sim 1190 \text{ cm}^{-1}$ is observed to decrease with increasing γ -ray dose until 35 kGy of gamma radiation (Table 4). This can be attributed to further dissociation of LiBOB into ions. When the γ -dose is increased beyond 35 kGy, ion association takes place at a faster rate and the area and the intensity of the LiBOB peak increased. This is also supported by FTIR deconvolution results as will be seen later.

Fig. 6. FTIR deconvolution of PVDF-LiBOB electrolyte with (a) 0, (b) 10, (c) 25, (d) 35, (e) 40 and (f) 50 kGy γ -ray doses at band between 1220 and 1135 cm^{-1} .

Table 4. Area and intensity (in a.u.) of FTIR band at 1190 cm^{-1} due to C-O valence out-of phase of LiBOB salt.

Peng and Wu [30] reported that the vibrational band corresponding to the amorphous nature of PVDF can be observed at 904 cm^{-1} . In this work, the band at 904 cm^{-1} has shifted to

876 cm^{-1} . Fig. 7 shows the FTIR band between 905 and 850 wavenumbers. The area and intensity of this band for every gamma dose are listed in Table 5. It is observed that the sample irradiated with 35 kGy γ -rays have the largest area and highest intensity compared to other samples. This indicates that the sample exposed to 35 kGy γ -rays is the most amorphous sample, thus further strengthening the results estimated from DSC and XRD.

Fig. 7. FTIR spectra of PVDF-LiBOB electrolyte with (a) 0, (b) 10, (c) 25, (d) 35, (e) 40 and (f) 50 kGy γ -ray doses at band between 905 and 850 cm^{-1} .

Table 5. Area and intensity of FTIR band between 905 and 850 cm^{-1} of PVDF-LiBOB with different gamma radiation doses.

Fig. 8 shows the deconvolution of the FTIR spectra in the absorbance mode for all samples. The deconvoluted peaks are assigned following the report by Holomb et. al [33]. In Fig. 8, the band of free ions is observed at 1804 cm^{-1} and the band at 1812 cm^{-1} is due to contact ions of LiBOB salt [33]. The area percentages of free ions and contact ions can be calculated from the ratio of the free or contact ions area to the total area of deconvolution peaks, respectively. Table 6 lists the percentage of free ions and contact ions of PVDF-LiBOB electrolyte after exposure to different gamma irradiation doses. The results are seen to support the change in LiBOB peak area of Fig. 6.

Fig. 8. FTIR deconvolution of PVDF-LiBOB electrolyte with (a) 0, (b) 10, (c) 25, (d) 35, (e) 40 and (f) 50 kGy γ -ray doses.

Table 6. Area percentage of free and contact ions of PVDF-LiBOB electrolyte with different gamma irradiation

It is observed that the percentage of free ions in the electrolyte increased up to the sample irradiated with 35 kGy γ -rays. This imply that irradiation of gamma ray into the electrolytes causes more ions to dissociate, thus help for ion conduction. Beyond 35 kGy gamma irradiation, the percentage of free ions is observed to decrease. This may be attributed to ion association.

3.4 Impedance spectroscopy (IS)

The bulk impedance, R_b was extracted from the Nyquist plots. A typical set of Nyquist plots for samples irradiated with different gamma doses is shown in Fig. 9. The bulk impedance decreased with increasing the γ -doses, and the lowest was recorded for the sample irradiated with 35 kGy γ -rays. The DC conductivity of PVDF-LiBOB polymer electrolyte with different γ doses is plotted as in Fig. 10. The non-irradiated sample has the lowest room temperature conductivity of $2.01 \times 10^{-5} \text{ S cm}^{-1}$. On irradiating the sample with 10 kGy γ -rays, conductivity increased to $2.30 \times 10^{-4} \text{ S cm}^{-1}$ (about one magnitude order). The conductivity gradually increased with increasing γ -ray doses up to $3.05 \times 10^{-4} \text{ S cm}^{-1}$ for sample irradiated with 35 kGy γ -rays. The conductivity is observed to decrease on exposure to higher γ doses. Compared to the non-irradiated sample, there is an overall increase in conductivity on irradiation as shown in Table 7.

Fig. 9. Nyquist plot of PVDF-LiBOB electrolyte irradiated with different γ -radiation doses at room temperature.

Fig. 10. The conductivity of PVDF-LiBOB electrolyte irradiated with different γ -radiation doses.

The variation of conductivity can be related with number density (n), mobility (μ) and diffusion coefficient (D) of charge carriers in the electrolyte. From the percentage variation of free ions with respect to amount of dose obtained from FTIR deconvolution, the number density

(n), mobility (μ) and diffusion coefficient (D) of charge carriers can be calculated using the equations (4-6) [34].

$$n = \frac{M \times N_A}{V_{Total}} \times \text{free ions (\%)} \quad (4)$$

$$\mu = \frac{\sigma}{ne} \quad (5)$$

$$D = \frac{\mu k_b T}{e} \quad (6)$$

The variation of number density (n), mobility (μ) and diffusion coefficient (D) of free or mobile ions with γ doses are shown in Fig. 11. The sample exposed to 35 kGy γ -rays exhibited the highest number density of mobile ions. This indicates that γ -irradiation have resulted in more free ions that can contribute to ionic conductivity. Samples irradiated with 40 and 50 kGy γ -rays showed a decrease in number density of free ions that could have taken part in crosslinking or the formation of contact ions and larger aggregates that do not contribute to conductivity [35]. This can be observed from the increasing of percentage of contact ions in FTIR.

Fig. 11. The variation of number density, mobility and diffusivity of charge carriers with different γ -doses.

Values for these parameters number density (n), mobility (μ) and diffusion coefficient (D) free or mobile ions are listed in Table 7. It can be understood that the ionic conductivity is closely related to the number density of mobile ions. γ -irradiation also influences ionic mobility and diffusion coefficient. It can be observed from Table 7 that conductivity variation with γ -ray doses is similar to the variation of n , μ and D with increasing γ -ray doses. Hence, it can be inferred that γ -irradiation of PVDF based electrolyte increased the dissociation of salt resulting

in increased number density of mobile ions, formed more amorphous phases leading to increased ionic mobility and diffusion coefficient of the mobile ions. Irradiating the electrolyte with greater than 35 kGy γ -radiation decreased the three parameters. This could be attributed to ion association that led to increased crystallinity and glass transition temperature.

Table 7. Calculated transport parameters of PVDF-LiBOB electrolyte with different gamma irradiation

The frequency variation of the real part of AC conductivity is shown in Fig. 12 for different doses at room temperature. From Fig. 12, three frequency regions can be observed. The regions are low frequency dispersion region, frequency independent plateau region and high frequency region. The low-conductivity value at low frequencies dispersion region is related to the accumulation of ions due to the slow periodic reversal of the electric field [36]. The intermediate region corresponds to the frequency independent plateau region from which the room temperature conductivity can be obtained [37] and the high frequency dispersion region corresponding to bulk relaxation phenomenon. The DC ionic conductivity has been calculated by extrapolating the plateau region to the vertical axis for each dose of the polymer electrolyte. The maximum conductivity obtained from Fig. 12 is compatible with earlier reported in Fig. 11.

Fig. 12. The A.C. conductivity versus frequency of PVDF-LiBOB electrolyte at different γ -radiation doses.

Table 8. An extrapolated graph of $\log(\sigma)$ ac versus \log frequency

4. Conclusions

We obtained the results of PVDF-LiBOB polymer electrolyte films that were irradiated with γ -radiation to study the modification in ion conductivity induced by irradiation. The maximum conductivity was obtained for the sample irradiated with 35 kGy γ -rays which exhibited ionic conductivity $3.05 \times 10^{-4} \text{ S cm}^{-1}$. From the fourier transform infrared spectrum, each irradiated sample has been deconvoluted in the wavenumber region between 1830 and 1758 cm^{-1} in order to estimate the percentage of free and contact ions in the samples. The number density (n), mobility (μ) and diffusion coefficient (D) of the irradiated samples were found to increase with increase γ -ray doses up to 35 kGy. Beyond this dose, values of three parameters decreased. Sample irradiated with 35 kGy γ -rays is the most amorphous, represented by lowest degree of crystallinity (χ_c), glass transition temperature (T_g) and melting temperature (T_m). Since the 35 kGy γ -irradiated sample is most amorphous, the ions are easier to flow in this electrolyte thus increase the conductivity.

Acknowledgments

The HIRG grant No. J-00000-73555 awarded by the University of Malaya is greatly appreciated and acknowledged.

Figure captions

- Fig. 1.** The melting point, T_m peaks of PVDF-LiBOB electrolyte with different γ -radiation doses. Inset figure exhibits the DSC of PVDF-LiBOB polymer electrolyte in full scale cycles.
- Fig. 2.** Glass transition temperature, T_g of PVDF-LiBOB electrolyte with (a) 0, (b) 10, (c) 25, (d) 35, (e) 40 and (f) 50 kGy γ -irradiation.
- Fig. 3.** XRD patterns of (a) LiBOB salt and PVDF-LiBOB electrolyte with PVDF-LiBOB electrolyte with (b) 0, (c) 10, (d) 25, (e) 35, (f) 40 and (g) 50 kGy γ -irradiation.
- Fig. 4.** XRD deconvolution of PVDF-LiBOB electrolyte with (a) 0, (b) 10, (c) 25, (d) 35, (e) 40 and (f) 50 kGy γ -irradiation.
- Fig. 5.** FTIR Spectra of PVDF-LiBOB electrolyte with different γ -doses.
- Fig. 6.** FTIR deconvolution of PVDF-LiBOB electrolyte with (a) 0, (b) 10, (c) 25, (d) 35, (e) 40 and (f) 50 kGy γ -ray doses at band between 1220 and 1135 cm^{-1} .
- Fig. 7.** FTIR spectra of PVDF-LiBOB electrolyte with (a) 0, (b) 10, (c) 25, (d) 35, (e) 40 and (f) 50 kGy γ -ray doses at band between 905 and 850 cm^{-1} .
- Fig. 8.** FTIR deconvolution of PVDF-LiBOB electrolyte with (a) 0, (b) 10, (c) 25, (d) 35, (e) 40 and (f) 50 kGy γ -ray doses.
- Fig. 9.** Nyquist plot of PVDF-LiBOB electrolyte irradiated with different γ -radiation doses at room temperature.
- Fig. 10.** The conductivity of PVDF-LiBOB electrolyte irradiated with different γ -radiation doses.
- Fig. 11.** The variation of number density, mobility and diffusivity of charge carriers with different γ -doses.
- Fig. 12.** The A.C. conductivity versus frequency of PVDF-LiBOB electrolyte at different γ -radiation doses.

Table captions

- Table 1.** T_g , T_m , ΔH_m and χ_c values of PVDF-LiBOB electrolytes with different γ -radiation doses from DSC.
- Table 2.** A_c , A_a and χ_c values of PVDF-LiBOB electrolytes with different γ -radiation doses from XRD.
- Table 3.** The main FTIR peaks of PVDF-LiBOB and their possible assignments.
- Table 4.** Area and intensity (in a.u.) of FTIR band at 1190 cm^{-1} due to C-O valence out-of phase of LiBOB salt.
- Table 5.** Area and intensity (in a.u.) of FTIR band between 905 and 850 cm^{-1} for PVDF-LiBOB with different γ -radiation doses.
- Table 6.** Area percentage of free and contact ions of PVDF-LiBOB electrolyte with different γ -irradiation.
- Table 7.** Calculated transport parameters of PVDF-LiBOB electrolyte with different γ -irradiation.
- Table 8.** An extrapolated graph of $\log(\sigma)$ ac versus \log frequency.

References

- [1] O. Saito, in *The Radiation Chemistry of Macromolecules*, ed. M. Dole, Academic Press, New York, 1972, p 223.
- [2] M. Sinha, M.M. Goswami, D. Mal, T.R. Middya, S. Tarafdar, U. De, S.K. Chaudhuri and D. Das, *Ionics*, 2008, 14, 323-327.
- [3] D. Finka, W. H. Chungae, R. Kletta, A. Schmoldta, J. Cardosob, R. Montielb, M. H. Vazquezb, L. Wangc, F. Hosoid, H. Omichid and P.G.-Langerd, *Radiat. Eff. Defect. S.*, 1995, 133, 193-208.
- [4] D. Fink, R. Klett, L. T. Chadderton, J. Cardoso, R. Montiel, H. Vazquez, and A. A. Karanovich, *Nucl. Instrum. Meth. B.*, 1996, 111, 303-314.
- [5] M. F. Zaki, *J. Phys. D. Appl. Phys.*, 2008, 41, 175404.
- [6] D. Sinha, K. L. Sahoo, U. B. Sinha, T. Swu, A. Chemseddine and D. Fink, *Radiat. Eff. Defect. S.*, 2004, 159, 587-595.
- [7] G. Kecskemeti, T. Smausz, N. Kresz, Zs. Toth, B. Hopp, D. Chrisey and O. Berkesi, *Appl. Surf. Sci.*, 2006, 253, 1185-1189.
- [8] A. M. Basha, M. A. Ahmed, H. K. Marey and T. A. Hanafy, *Indian J. Phys.*, 1996, 70A, 619-625.
- [9] M. A. Ahmed, A. M. Basha, H. K. Marey and T. A. Hanafy, *J. Appl. Polym. Sci.*, 2001, 79, 1749-1755.
- [10] T. A. Hanafy, *Curr. Appl. Phys.*, 2008, 8, 527-534.
- [11] G. Boiteux, J. F. Chailan, J. Chauchard and G. Seytre, *Nucl. Instrum. Meth. B.*, 1997, 131, 172-179.
- [12] M. E. M-. Pardo, J. Cardoso, H. Vazquez and M. Aquilar, *Nucl. Instrum. Meth. B.*, 1998, 140, 325-340.
- [13] T. Phukan, D. Kanjilal, T. D. Goswami and H. L. Das, *Nucl. Instrum. Meth. B.*, 1999, 155, 116-119.
- [14] E. Neagu, P. Pissis, L. Apeki and J. L. G. Ribelles, *J. Phys. D. Appl. Phys.*, 1997, 30, 1551-1560.
- [15] L. Calcagno, G. Compagnini and G. Foti, *Nucl. Instrum. Meth. B.*, 1992, 65, 413-422.
- [16] N. G. McCrum, B. E. Read and G. William, *An Elastic and Dielectric Effects in Polymeric Solids*, (1967) John Wiley, New York. (pp. 501-520).
- [17] R. Kumar, S. A. Ali, U. De, D. K. Avasthi and R. Prasad, *Indian J. Phys.*, 2009, 83, 963-968.
- [18] R. C. Abul-Hail, *J. Basrah Researches (Sci.)*, 2010, 36, 6.
- [19] F. B. Dias, L. Plomp and J. B. J. Veldhuis, *J. Power Sources*, 2000, 88, 169-191.
- [20] V. Aravindan and P. Vickraman, *Polym. Eng. Sci.*, 2009, 49, 2109-2115.
- [21] J. C. Li, C. L. Wang, W. L. Zhong, P. L. Zhang, Q. H. Webb and J. F. Webb, Vibrational mode analysis of β -phase poly(vinylidene fluoride), *Appl. Phys. Lett.*, 2002, 81, 2223-2225.
- [22] S. R. Elliott, *Adv. Phys.*, 1987, 36, 135-217.
- [23] T. Czvikovszky and H. Hargitai, *Radiat. Phys. Chem.*, 1999, 55, 727-730.
- [24] A. Ghosh and A. Pan, *Phys. Rev. Lett.*, 2000, 84, 2188-2190.
- [25] M. Hema, S. Selvasekerapandian, G. Hirankumar, A. Sakunthala, D. Arunkumar and H. Nithya, *J. Phys. Chem. Solids*, 2009, 70, 1098-1103.
- [26] K. J. Zeleznak and R. C. Hosene, The glass transition in starch, *Cereal Chem.*, 1987, 64, 121-124.

- [27] M. M. Noor, M. A. Careem, S. R. Majid and A. K. Arof, *Mater. Res. Innov.*, 2011, 15, 157-160.
- [28] S. Wang, W. Qiu, T. Li, B. Yu and H. Zhao, *Inter. J. Electrochem. Sci.*, 2006, 1, 250-257.
- [29] N. Terinte, R. Ibbett and K. C. Schuster, *Lenzinger Berichte*, 2011, 89, 118.
- [30] Y. Peng and P. Wu, *Polymer*, 2004, 45, 5295–5299.
- [31] B. Ahmed, S. K. Raghuvanshi, Siddhartha, N. P. Sharma, J. B. M. Krishna and M. A. Wahab, *Prog. Nanotechno. Nanomater.*, 2013, 2, 42-46.
- [32] M. Li, H.J. Wondergem, M.-J. Spijkman, K. Asadi, I. Katsouras, P.W.M. Blom and D.M. de Leeuw, Revisiting the δ -phase of poly(vinylidene fluoride) for solution-processed ferroelectric thin films, *Nat. Mater.*, 2013, 12, 433-438.
- [33] R. Holomb, W. Xu, H. Markusson, P. Johansson and P. Jacobsson, *J. Phys. Chem. A*, 2006, 110, 11467-11472.
- [34] A. K. Arof, S. Amirudin, S. Z. Yusof, and I. M. Noor, *Phys. Chem. Chem. Phys.*, 2014, 16, 1856–1867.
- [35] I. S. Noor, S. R. Majid and A. K. Arof, *Electrochim. Acta*, 2013, 102, 149– 160.
- [36] A. S. A. Khair, R. Puteh and A. K. Arof, *Physica B*, 2006, 373, 23–27.
- [37] E. Barsoukov and J. R. Macdonald, Impedance spectroscopy, theory experiment and applications, Wiley-Interscience, (2005) New York.

Figures

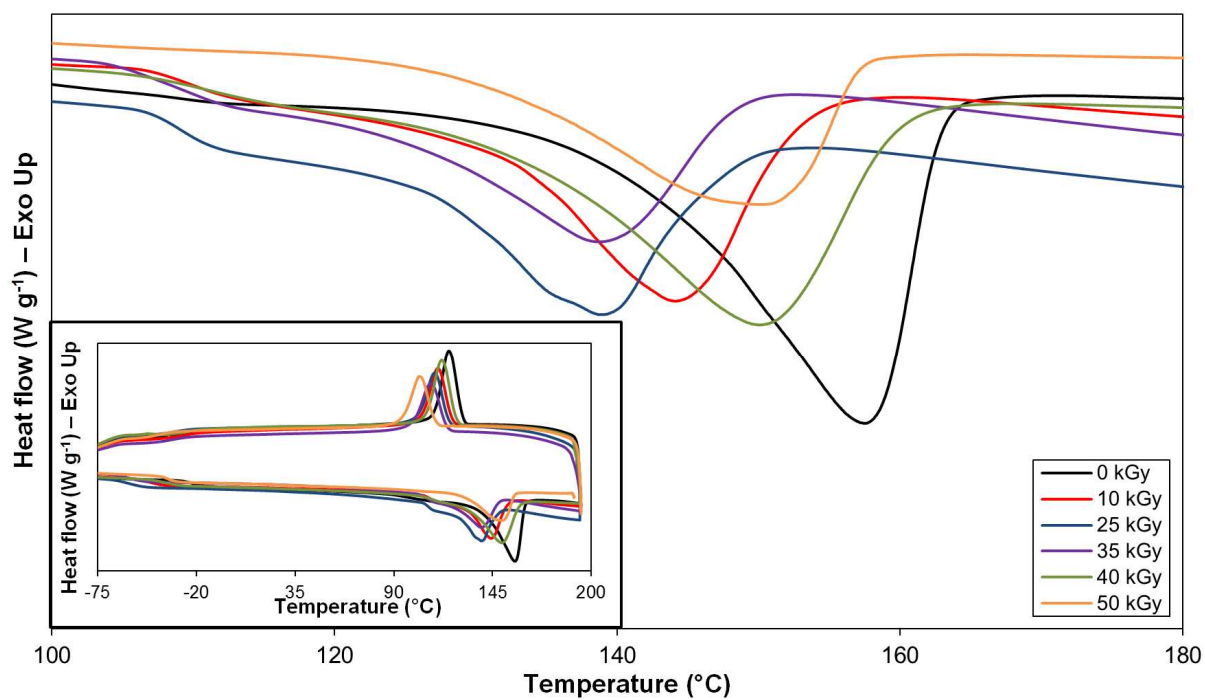


Fig. 1. The melting point, T_m peaks of PVDF-LiBOB electrolyte with different γ -radiation doses. Inset figure exhibits the DSC of PVDF-LiBOB polymer electrolyte in full scale cycles.

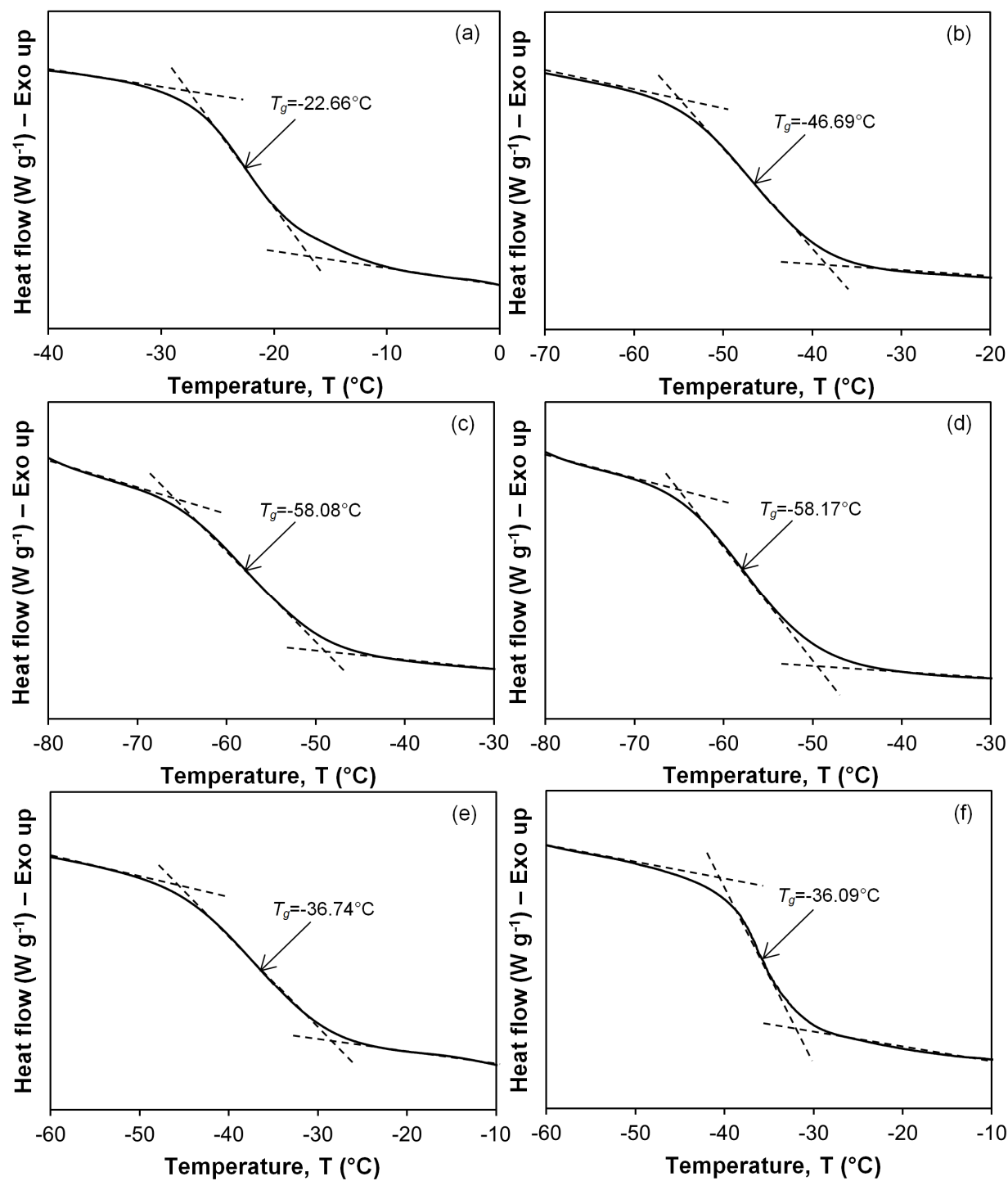


Fig. 2. Glass transition temperature, T_g of PVDF-LiBOB electrolyte with (a) 0, (b) 10, (c) 25, (d) 35, (e) 40 and (f) 50 kGy γ -irradiation.

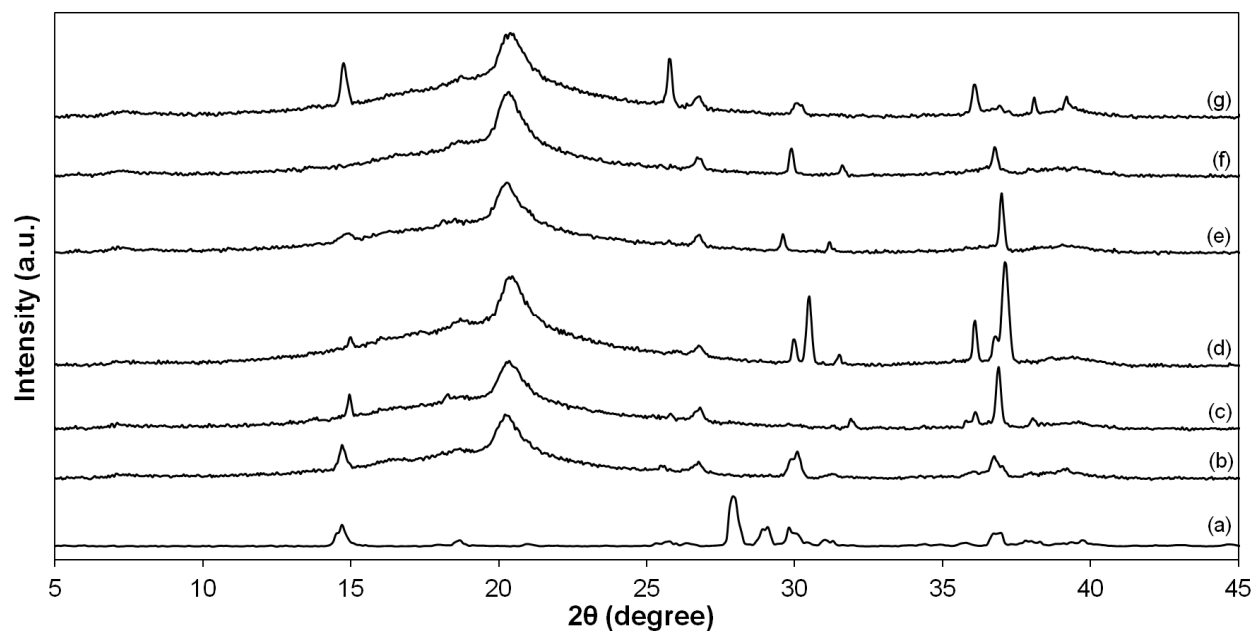


Fig. 3. XRD patterns of (a) LiBOB salt and PVDF-LiBOB electrolyte with PVDF-LiBOB electrolyte with (b) 0, (c) 10, (d) 25, (e) 35, (f) 40 and (g) 50 kGy γ -irradiation.

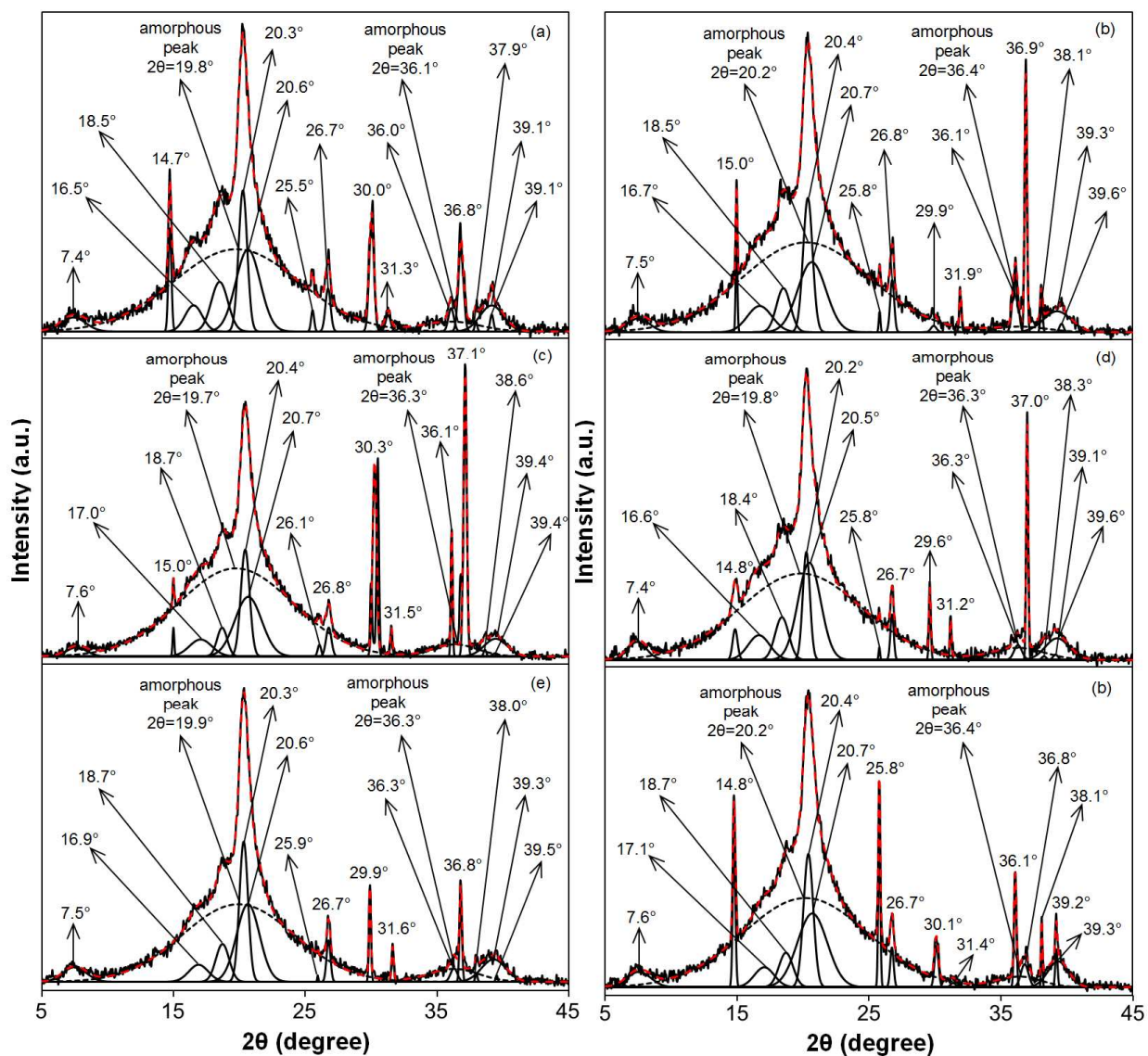


Fig. 4. XRD deconvolution of PVDF-LiBOB electrolyte with (a) 0, (b) 10, (c) 25, (d) 35, (e) 40 and (f) 50 kGy γ -irradiation.

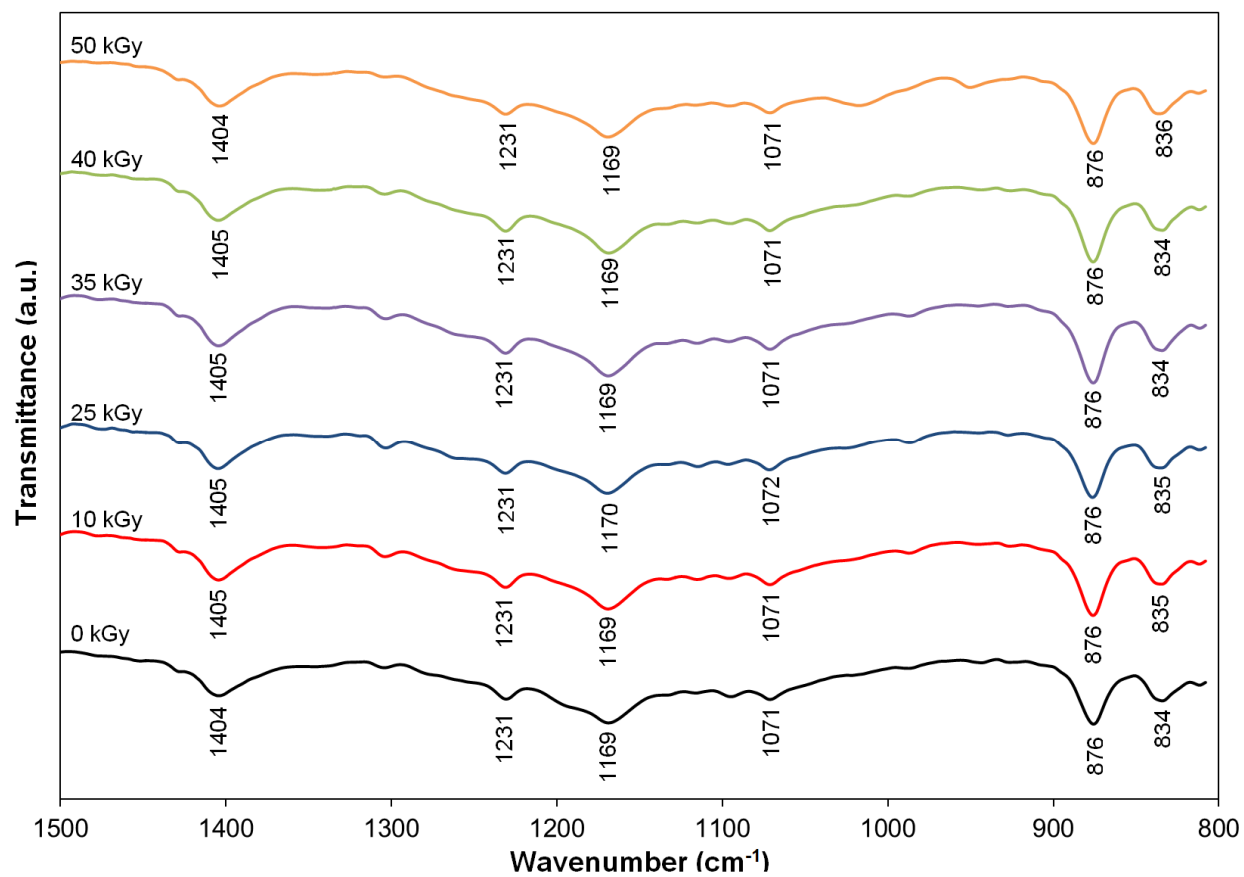


Fig. 5. FTIR Spectra of PVDF-LiBOB electrolyte with different γ -doses.

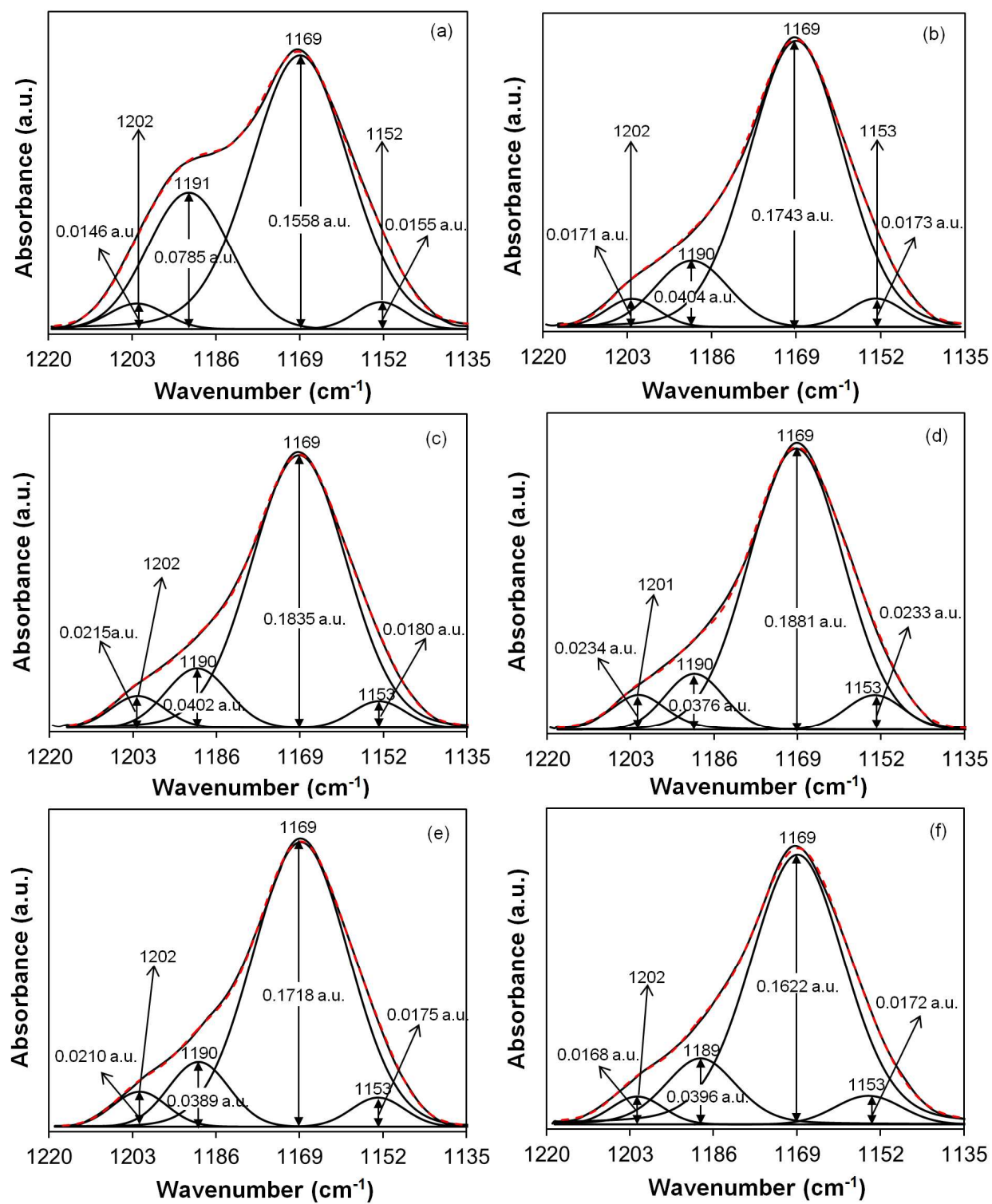


Fig. 6. FTIR deconvolution of PVDF-LiBOB electrolyte with (a) 0, (b) 10, (c) 25, (d) 35, (e) 40 and (f) 50 kGy γ -ray doses at band between 1220 and 1135 cm^{-1} .

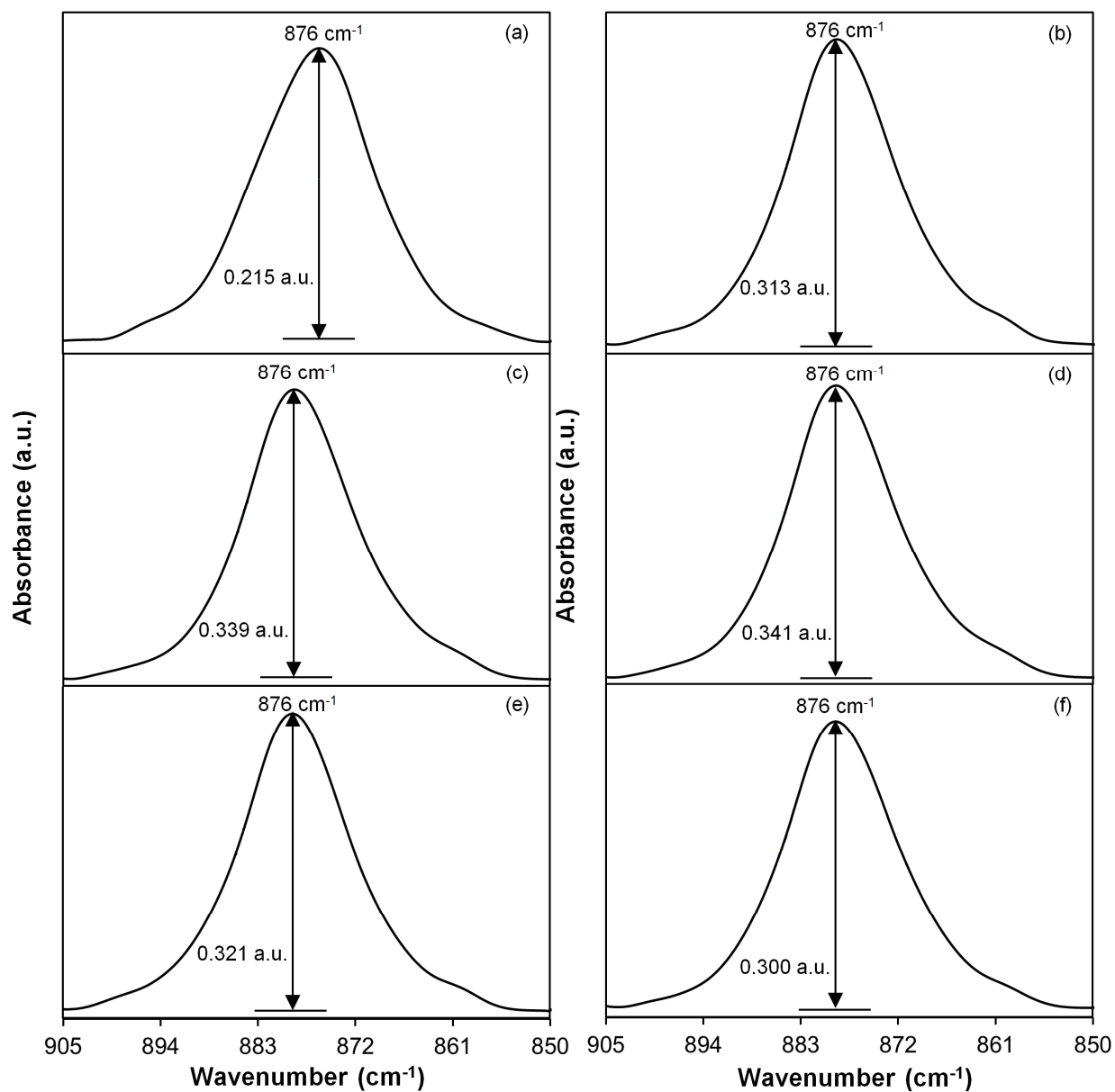


Fig. 7. FTIR spectra of PVDF-LiBOB electrolyte with (a) 0, (b) 10, (c) 25, (d) 35, (e) 40 and (f) 50 kGy γ -ray doses at band between 905 and 850 cm^{-1} .

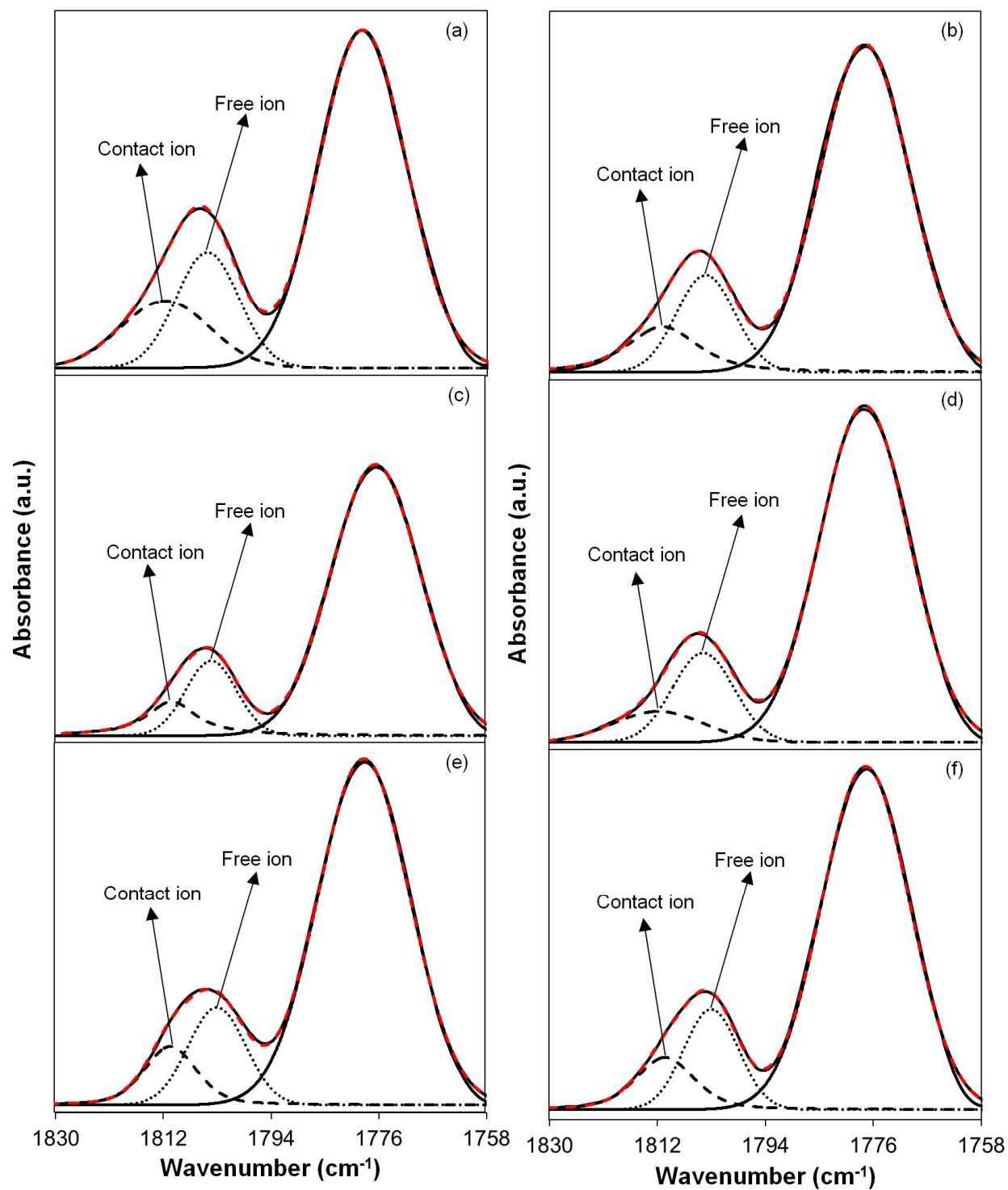


Fig. 8. FTIR deconvolution of PVDF-LiBOB electrolyte with (a) 0, (b) 10, (c) 25, (d) 35, (e) 40 and (f) 50 kGy γ -ray doses.

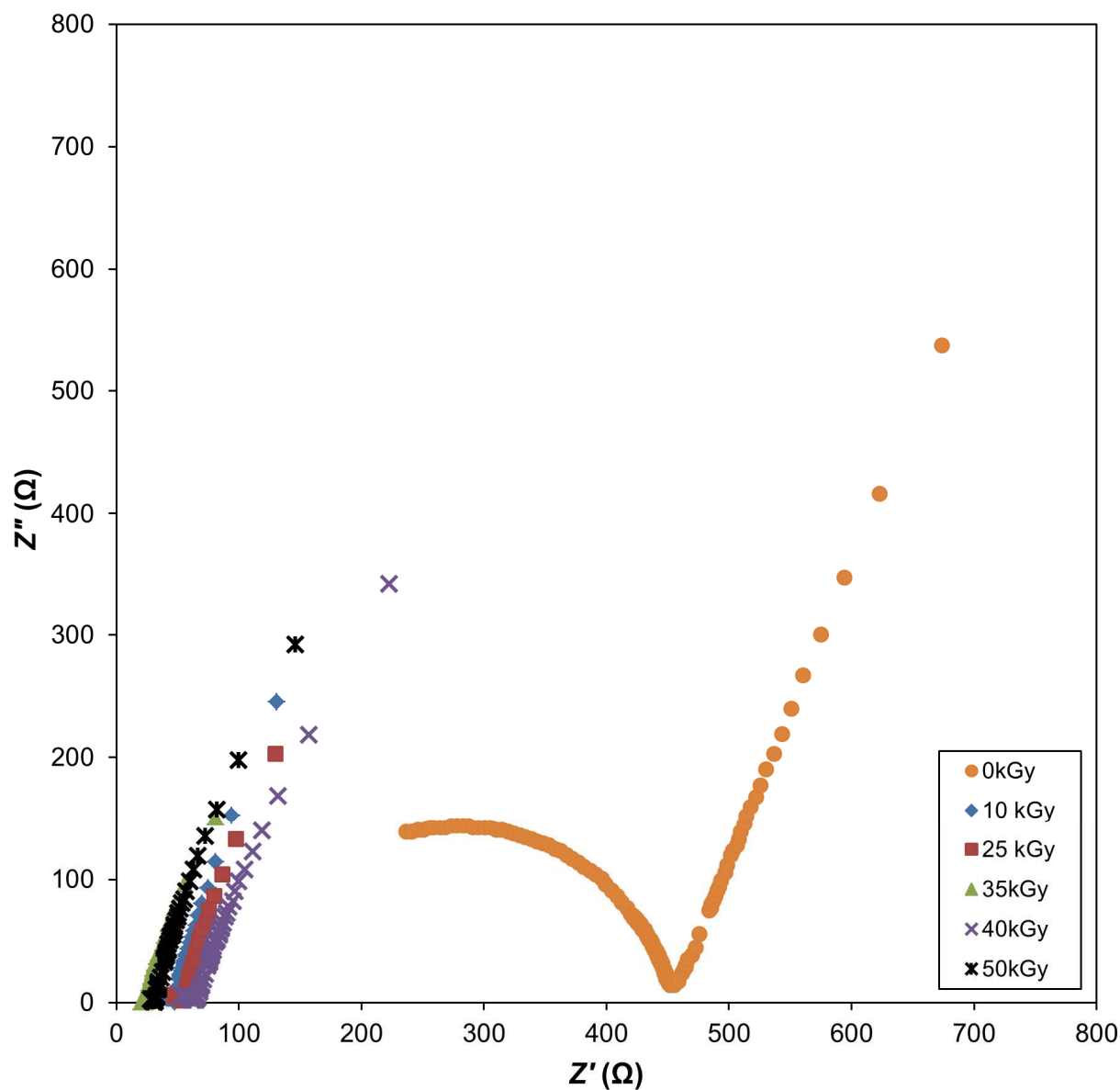


Fig. 9. Nyquist plot of PVDF-LiBOB electrolyte irradiated with different γ -radiation doses at room temperature.

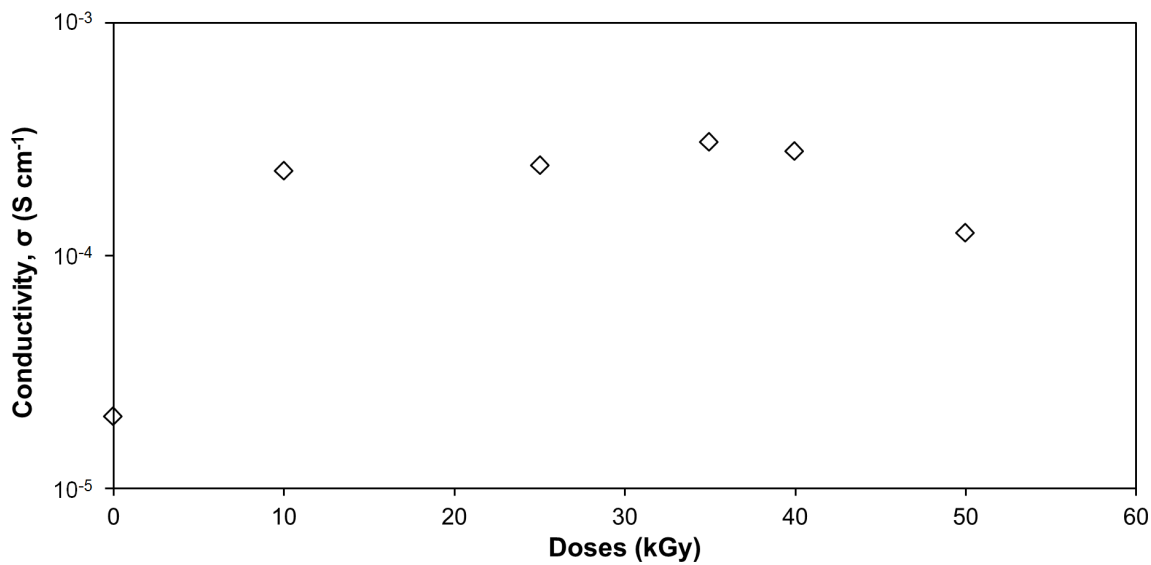


Fig. 10. The conductivity of PVDF-LiBOB electrolyte irradiated with different γ -radiation doses.

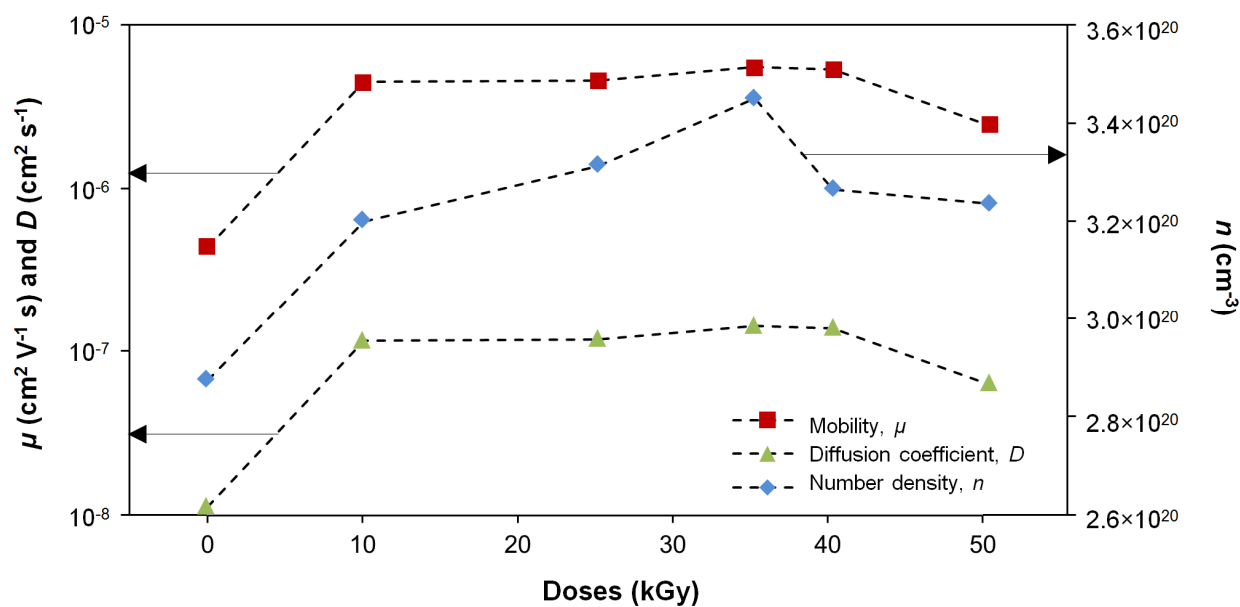


Fig. 11. The variation of number density, mobility and diffusivity of charge carriers with different γ -doses.

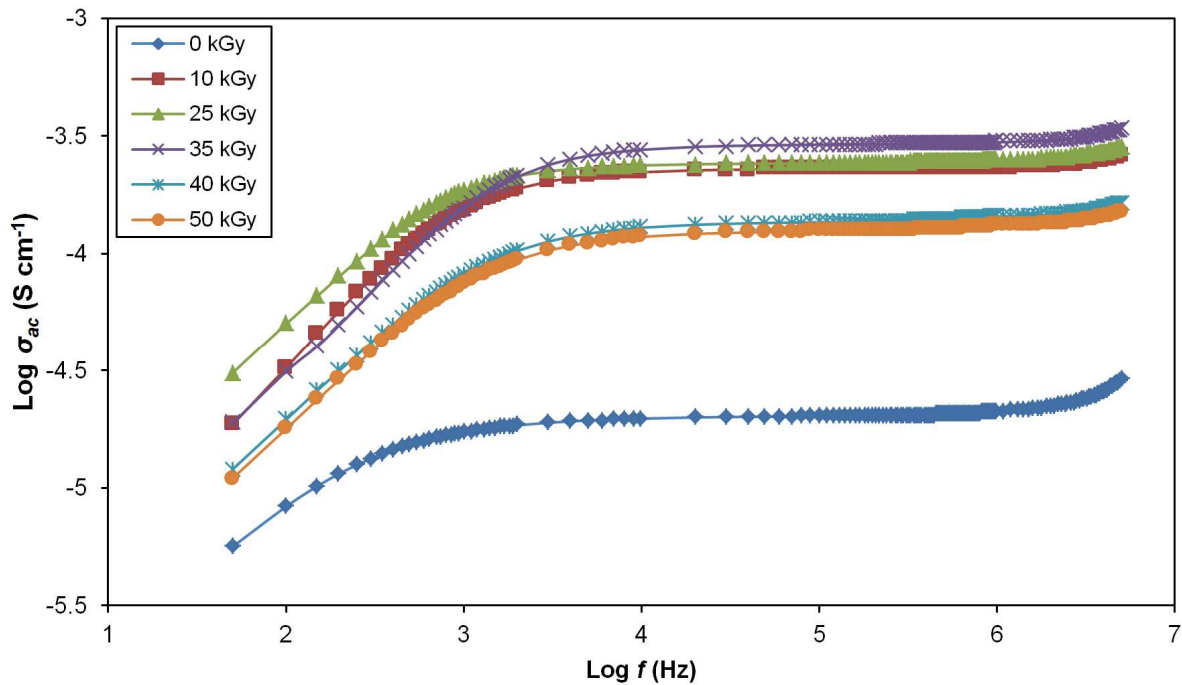


Fig. 12. The A.C. conductivity versus frequency of PVDF-LiBOB electrolyte at different γ -radiation doses.

Tables

Table 1. T_g , T_m , ΔH_m and χ_c values of PVDF-LiBOB electrolytes with different γ -radiation doses from DSC.

| Dose (kGy) | T_g (°C) | T_m (°C) | ΔH_m (J g ⁻¹) | χ_c (%) |
|------------|------------|------------|-----------------------------------|--------------|
| 0 | -22.66 | 157.5 | 777.1 | 100.0 |
| 10 | -46.69 | 144.1 | 482.4 | 62.1 |
| 25 | -58.08 | 139.0 | 358.1 | 46.1 |
| 35 | -58.17 | 138.7 | 350.9 | 45.2 |
| 40 | -36.74 | 149.9 | 440.7 | 56.7 |
| 50 | -36.09 | 150.1 | 443.5 | 57.1 |

T_g = glass transition temperature, T_m = melting temperature, ΔH_m = enthalpy of melting, and χ_c = degree of crystallinity.

Table 2. A_c , A_a and χ_c values of PVDF-LiBOB electrolytes with different γ -radiation doses from XRD.

| Doses (kGy) | A_c | A_a | χ_c (%) |
|-------------|---------|---------|--------------|
| 0 | 3208.83 | 4774.66 | 40.19 |
| 10 | 3317.62 | 5623.12 | 37.11 |
| 25 | 4470.59 | 7927.34 | 36.06 |
| 35 | 3070.27 | 5628.83 | 35.29 |
| 40 | 3279.43 | 5591.13 | 36.97 |
| 50 | 4108.89 | 6891.66 | 37.35 |

A_c = Area of crystalline region, A_a = Area of amorphous region, and χ_c = degree of crystallinity.

Table 3. The main FTIR peaks of PVDF-LiBOB and their possible assignments.

| Wavenumber (cm ⁻¹) | Assignments |
|--------------------------------|---|
| 834 | $\nu_a(\text{CF}_2)$ of PVDF |
| 876 | $\nu_a(\text{C-C})$ and $\nu_s(\text{CF}_2)$ of PVDF |
| 1071 | $\nu_a(\text{C-C})$, $w(\text{CF}_2)$ and $w(\text{CH}_2)$ of PVDF |
| 1169 | $\nu_s(\text{CF}_2)$ and $t(\text{CH}_2)$ of PVDF |
| 1231 | $\nu_a(\text{CF}_2)$ and $[w(\text{CH}_2)]$ of PVDF |
| 1404 | $w(\text{CH}_2)$ and $\nu_a(\text{C-C})$ of PVDF |

ν_s = symmetrical stretching, ν_a = asymmetrical stretching, w = wagging and t = torsional,

Table 4. Area and intensity (in a.u.) of FTIR band at 1190 cm^{-1} due to C-O valence out-of phase of LiBOB salt.

| Doses (kGy) | Area (unit^2) | Intensity (a.u.) |
|-------------|--------------------------|------------------|
| 0 | 1.6340 | 0.0785 |
| 10 | 0.7399 | 0.0404 |
| 25 | 0.6400 | 0.0402 |
| 35 | 0.5600 | 0.0376 |
| 40 | 0.6000 | 0.0389 |
| 50 | 0.7479 | 0.0396 |

Table 5. Area and intensity (in a.u.) of FTIR band between 905 and 850 cm^{-1} for PVDF-LiBOB with different γ -radiation doses.

| Doses (kGy) | Area (unit^2) | Intensity (a.u.) |
|-------------|--------------------------|------------------|
| 0 | 3.8 | 0.215 |
| 10 | 5.2 | 0.313 |
| 25 | 5.6 | 0.339 |
| 35 | 5.7 | 0.341 |
| 40 | 5.4 | 0.321 |
| 50 | 5.1 | 0.300 |

Table 6. Area percentage of free and contact ions of PVDF-LiBOB electrolyte with different γ -irradiation

| Doses (kGy) | Free ions (%) | Contact ions (%) |
|-------------|---------------|------------------|
| 0 | 55.18 | 44.82 |
| 10 | 61.44 | 38.56 |
| 25 | 63.61 | 36.39 |
| 35 | 66.26 | 33.74 |
| 40 | 62.69 | 37.31 |
| 50 | 62.13 | 37.87 |

Table 7. Calculated transport parameters of PVDF-LiBOB electrolyte with different γ -irradiation

| Doses (kGy) | Conductivity, σ (S cm^{-1}) | n ($\times 10^{20}\text{ cm}^{-3}$) | μ ($\times 10^{-6}\text{ cm}^2\text{ V}^{-1}\text{ s}$) | $n\mu$ ($\times 10^{15}\text{ cm}^{-1}\text{ V}^{-1}\text{ s}$) | D ($\times 10^{-7}\text{ cm}^2\text{ s}^{-1}$) |
|-------------|---|---|---|---|--|
| 0 | 2.01×10^{-5} | 2.87 | 0.44 | 0.13 | 0.11 |
| 10 | 2.30×10^{-4} | 3.20 | 4.49 | 1.44 | 1.15 |
| 25 | 2.43×10^{-4} | 3.31 | 4.58 | 1.52 | 1.18 |
| 35 | 3.05×10^{-4} | 3.45 | 5.52 | 1.90 | 1.42 |
| 40 | 2.79×10^{-4} | 3.26 | 5.34 | 1.74 | 1.37 |
| 50 | 1.26×10^{-4} | 3.24 | 2.43 | 0.79 | 0.63 |

Table 8. An extrapolated graph of $\log(\sigma)$ ac versus \log frequency

| Doses (kGy) | Log (σ_{ac}) |
|-------------|-----------------------|
| 0 | -4.70 |
| 10 | -3.64 |
| 25 | -3.62 |
| 35 | -3.54 |
| 40 | -3.87 |
| 50 | -3.91 |